

## Observation of a Strongly Nested Fermi Surface in the Shape-Memory Alloy $\text{Ni}_{0.62}\text{Al}_{0.38}$

S. B. Dugdale, R. J. Watts, J. Laverock, Zs. Major, and M. A. Alam

*H. H. Wills Physics Laboratory, University of Bristol, Tyndall Avenue, Bristol BS8 1TL, United Kingdom*

M. Samsel-Czekala and G. Kontrym-Sznajd

*W. Trzebiatowski Institute of Low Temperature and Structure Research, Polish Academy of Sciences,  
P.O. Box 1410, 50-950 Wrocław 2, Poland*

Y. Sakurai and M. Itou

*Japan Synchrotron Radiation Research Institute, SPring-8, 1-1-1 Kouto, Mikazuki, Sayo, Hyogo 679-5198, Japan*

D. Fort

*School of Metallurgy and Materials, University of Birmingham, Birmingham B15 2TT, United Kingdom*

(Received 29 June 2005; published 1 February 2006)

The Fermi surface topology of the shape-memory alloy  $\text{Ni}_{0.62}\text{Al}_{0.38}$  has been determined using Compton scattering. A large area of this Fermi surface can be made to nest with other areas by translation through a vector of  $\approx 0.18[1, 1, 0](2\pi/a)$ , which corresponds to the wave vector associated with martensitic precursor phenomena such as phonon softening and diffuse streaking in electron diffraction patterns. This observation is compelling evidence that these phenomena are driven by the enhanced electron-lattice coupling due to the Fermi surface nesting.

DOI: [10.1103/PhysRevLett.96.046406](https://doi.org/10.1103/PhysRevLett.96.046406)

PACS numbers: 71.18.+y, 63.20.Kr, 71.20.Be

Smart alloys that exhibit shape-memory and superelastic phenomena have been deployed in a wide variety of applications ranging from actuators in aircraft wings to surgical instruments. However, an atomic-scale understanding of the origin of the martensitic transformation (MT), the structural transformation at the heart of these phenomena, is still lacking. It has been hypothesized that lattice vibrations are the key, an idea supported by first-principles calculations indicating that strong coupling of certain phonons to the electrons (phonon softening), due to particular features in the Fermi surface, plays a crucial role [1–6]. Owing principally to the compositional disorder inherent to many of these alloys, a Fermi surface determination in these materials is experimentally challenging, with traditional quantum oscillatory techniques suffering due to their reliance on a long electronic mean-free path. Recent de Haas–van Alphen experiments in the austenitic phase of the low-temperature shape-memory alloy AuZn have reported an orbit whose cross-sectional area is in excellent agreement with first-principles calculations that predict the presence of a strongly nested sheet of Fermi surface [7]. In this Letter we provide experimental evidence in support of the intimate relationship between the phonon softening and the Fermi surface through a Compton scattering study of the shape-memory alloy  $\text{Ni}_{0.62}\text{Al}_{0.38}$ .

It is more than a century since Martens' exploration of the microstructure of steels gave the first insight into the origin of their macroscopic properties, and subsequently led to his name being associated with a more general solid-state phase transformation [8]. While metallurgists have a precise, albeit phenomenological, definition of a MT, and

physicists use the term more loosely to define many first-order transitions with acoustic anomalies, both disciplines generally agree that they are purely structural, diffusionless (meaning no atom-by-atom jumping within the unit cell), displacive (meaning a coordinated displacement of the atoms over distances much less than the atomic spacing) solid-solid phase transitions [9]. However, MTs have continued to fascinate generations of scientists.  $\text{Ni}_x\text{Al}_{1-x}$  alloys are well known to exhibit a MT for  $x \sim 0.62$  [1], and represent a prototypical compound for the transformation that is intermediate between weakly (almost second order) and strongly first order.

Early attempts to understand these transformations suggested that a phonon would become unstable at a particular temperature, at which point the lattice would displace spontaneously to a finite amplitude [10,11]. This “soft-mode” theory, however, is found to be lacking in several key aspects [12], which include (i) the observation that the phonon frequencies soften only slightly, and do not indicate harmonic instability, (ii) the prediction of a second-order transition, whereas in practice there is a finite, albeit small discontinuity in the microscopic order parameter (the static amplitude of the frozen-in soft mode), (iii) the empirical absence of critical fluctuations, and finally (iv) the presence of strong precursors of the new phase, or a distorted form of it, which persist well above the transition temperatures; examples of these precursors in the case of  $\text{Ni}_x\text{Al}_{1-x}$  include diffuse streaking in electron diffraction patterns and the corresponding “tweed” strain-contrast patterns in transmission electron microscope images, and anomalous softening of the transverse acoustic ( $\text{TA}_2$ ) pho-

non branch along  $[\xi\xi 0]$  at temperatures well above the MT [9,13]. These premartensitic phenomena have been associated with local deviations from the perfect cubic structure at temperatures well above the MT, the regions being formed as a result of the coupling of defect-induced strain fields and anomalous phonon softening.

It is well known that when parallel pieces of Fermi surface exist in a metal, there will be a strong electronic response at the wave vector which translates, or nests, one parallel piece onto the other. This role of the Fermi surface in influencing the electron-phonon coupling, was extensively investigated during the last two decades (see, for example, [14–16]), where premartensitic phenomena [9,13] were explicable in terms of Fermi surface nesting.

While anharmonic effects are thought to be responsible for the MT [17], it is Kohn anomalies [18] driven by nestable regions on the Fermi surface impacting on the electronic screening (and hence on the electron-phonon coupling) that were initially suggested as the origin of the premartensitic phenomena [1]. Given the disordered nature of the  $\text{Ni}_x\text{Al}_{1-x}$  alloys, the degree to which the Fermi surface remains a well-defined, sharp entity is an important consideration. Stocks *et al.* [19] tackled this issue by calculating the effect of disorder within the framework of the coherent potential approximation (CPA). They were able to show that, although there is significant smearing of the Fermi surface in many areas of the Brillouin zone (BZ), the region of the Fermi surface first identified by Zhao and Harmon [1] as exhibiting nesting (surprisingly, perhaps) remains rather sharp.

The key questions addressed here, however, are whether the actual Fermi surface of  $\text{Ni}_{0.62}\text{Al}_{0.38}$  resembles that predicted by *ab initio* calculation [1,19], and whether any nesting vector matches that of the strongly softened phonons. A previous attempt (also using Compton scattering) to establish a connection between the Fermi surface topology and any shape-memory behavior [20] was unsuccessful, principally due to the complexity of the Fermi surface of their  $\text{Ti}_{48.5}\text{Ni}_{51.5}$  alloy. Here, we present our measurement of the Fermi surface of  $\text{Ni}_{0.62}\text{Al}_{0.38}$  using the technique of Compton scattering [21].

In order to make a direct comparison with the Fermi surface predicted by band theory, we performed *ab initio* electronic structure calculations to reproduce the earlier work of Stocks *et al.* [19] for the disordered  $\text{Ni}_{0.62}\text{Al}_{0.38}$  alloy. We employed the fully relativistic Koringa-Kohn-Rostoker (KKR) method within the atomic sphere approximation, and the disorder was taken into account by the coherent potential approximation [22]. The lattice constant was taken to be 2.82 Å, and convergence was achieved at 816  $k$  points within the irreducible Brillouin zone. The Fermi surface was identified by the locus of the peaks in the Bloch spectral function,  $A^B(\mathbf{k}, \epsilon)$ . The sheet of (nestable) Fermi surface identified by Zhao and Harmon [1] is presented in Fig. 1, alongside the three-dimensional Fermi surface.

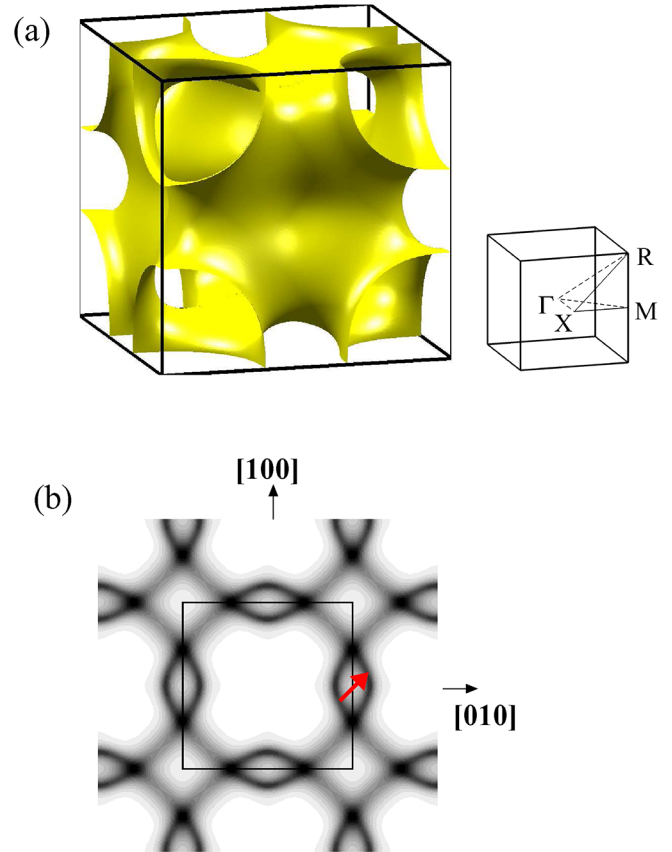


FIG. 1 (color online). (a) The Fermi surface of  $\text{Ni}_{0.68}\text{Al}_{0.32}$ , determined via the KKR calculation (shown alongside are the locations of some relevant symmetry points within the Brillouin zone), and (b) the intensity of the Bloch spectral function, where dark shades represent high intensity, of the sheet of Fermi surface proposed to accommodate the nesting in  $\text{Ni}_{0.68}\text{Al}_{0.32}$ , shown on the  $k_z = 0.48(\pi/a)$  plane. The Fermi surface can be identified as the strong oval features located on the edges of the Brillouin zone (the fainter lines being spectral weight from a band close to the Fermi energy). The arrow indicates the proposed nesting vector (along the  $[110]$  direction), and the edge of the first Brillouin zone is marked. Note that this sheet remains relatively sharp throughout the Brillouin zone, despite the disorder inherent to the system.

Our single crystal sample was cut by spark erosion from a single grain of a large ingot of  $\text{Ni}_{0.62}\text{Al}_{0.38}$  grown using the Bridgman method. It was subsequently annealed under argon at temperatures between 1230 and 1270 K for a total of 30 hours, followed by a vacuum degas at 900 K.

A total of 24 Compton profiles along different crystallographic directions were measured at room temperature on the high-resolution Compton spectrometer of beam line BL08W at the SPring-8 synchrotron [23,24]. This spectrometer is a Cauchois-type spectrometer, consisting of a Cauchois-type crystal analyzer and a position-sensitive detector, with a resolution FWHM at the Compton peak of 0.155 a.u. (1 a.u. of momentum =  $1.99 \times 10^{-24}$  kgms $^{-1}$ ) [23,24]. Whereas other Fermi surface techniques rely on a

long mean-free path of the electron or relatively defect-free crystal, Compton scattering is a robust technique insensitive to defects or disorder, providing a one-dimensional projection (double integral) of the underlying bulk electron momentum distribution. For each Compton profile,  $\sim 300\,000$  counts in the peak data channel were accumulated. Of the 24 Compton profiles that were collected, three were of high-symmetry directions, namely  $[100]$ ,  $[110]$ , and  $[111]$ , and ten were the “special directions” outlined by Kontrym-Sznajd *et al.* [25]; the remaining 11 Compton profiles were chosen in such a way so as to be equally spaced throughout the Brillouin zone. Each Compton profile was corrected for possible multiple-scattering contributions using a Monte Carlo method [26].

A three-dimensional momentum density was reconstructed [27] from this set of 24 profiles and then folded back into the first Brillouin zone using the Lock-Crisp-West procedure [28] to obtain the occupation density. The experimental Fermi surface (shown in Fig. 2) was extracted by contouring this density at a level fixed by an extremum in the first derivative along a direction where our calculations indicated the Fermi surface was likely to be well defined [29]. To illustrate that the reconstruction procedure does not introduce artifacts, the Fermi surface reconstructed from the Compton profiles calculated by the KKR method along the same 24 directions is shown in Fig. 3.

Before addressing the issue of how faithfully the *ab initio* calculations have described the observed Fermi surface, it is important to investigate the nesting properties of the experimentally determined one. A plane-by-plane inspection of the Fermi surface throughout the Brillouin

zone revealed that a vector  $\approx 0.18[1, 1, 0](2\pi/a)$  connects a large area in the manner predicted by Zhao and Harmon [1]. The plane through the BZ at  $k_z = 0.48(\pi/a)$ , for comparison with Fig. 1(b), is shown in Fig. 4.

We now return to the topology of the experimental Fermi surface and to the question of whether the *ab initio* calculations provide a good description of the Fermi surface for these materials. Clearly, the general shape of the experimental Fermi surface (Fig. 2) agrees well with the calculation (Fig. 1). As discussed above, the regions of Fermi surface responsible for the nesting are observed experimentally to be relatively flat. This, in conjunction with the large density of states (predicted by the calculations) spanning these wave vectors, provides a large propensity for nesting. There is, however, some noteworthy discrepancy between the calculated and experimental Fermi surfaces. Experimentally, a neck is observed to open around the  $X$  point of the Brillouin zone, whereas according to the calculations this sheet remains closed. The calculated band structure reveals flat (almost dispersionless) bands along  $X$ - $M$  and  $M$ - $R$  lying just below the Fermi level, leading to a van Hove singularity in the density of states at that energy. The opening up of a Fermi surface neck along  $\Gamma$ - $X$  implies that the Fermi level has crossed below this van Hove singularity and may be indicative of the impending lattice instability at the martensitic transformation (where the Fermi surface would undergo more substantial rearrangement).

In conclusion, we have presented the experimental Fermi surface of the disordered alloy  $\text{Ni}_{0.62}\text{Al}_{0.38}$  from the results of Compton scattering experiments, providing evidence in support of the intimate link between the elec-

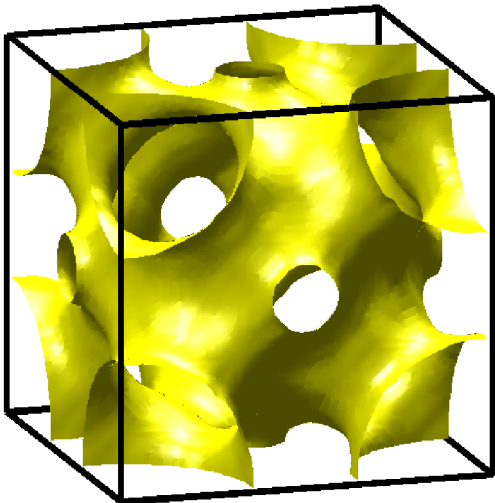


FIG. 2 (color online). The experimental Fermi surface of  $\text{Ni}_{0.68}\text{Al}_{0.32}$ , determined from the momentum density reconstruction of 24 Compton profiles along different crystallographic directions. The symmetry points are the same as those shown in Fig. 1.

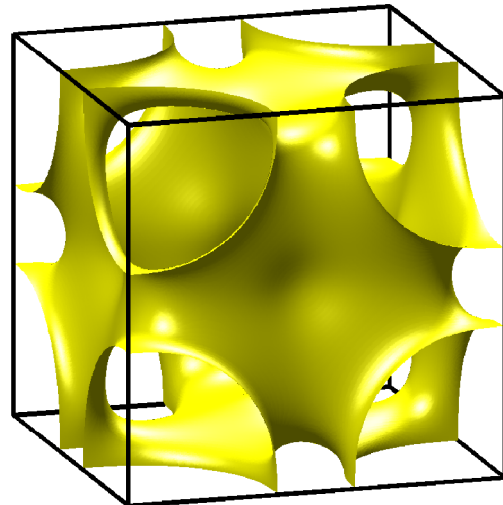


FIG. 3 (color online). The Fermi surface of  $\text{Ni}_{0.68}\text{Al}_{0.32}$ , determined from the momentum density reconstruction of 24 Compton profiles along different crystallographic directions calculated using the KKR method. The symmetry points are the same as those shown in Fig. 1.

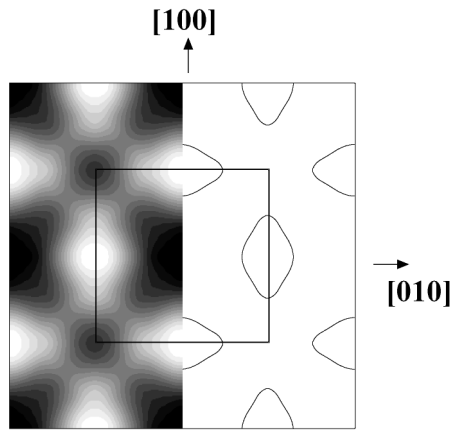


FIG. 4. A slice through the  $k_z = 0.48(\pi/a)$  plane of the experimental data, for comparison with Fig. 1(b). Shown on the left is the occupation density through this slice, where brighter shades represent a larger occupation. On the right is a contour of the occupation density at the level corresponding to the Fermi energy. The edge of the first Brillouin zone is marked.

tronic structure and the observed phonon softening. The Fermi surface obtained from *ab initio* calculations within the KKR-CPA framework has been shown to be in good agreement with the experimentally determined Fermi surface, with the exception of the opening of a neck along the  $X$  direction of the Brillouin zone. It is tentatively suggested that this topological disagreement may be explained by the proximity of the Fermi level to a van Hove singularity in the density of states.

We acknowledge the financial support of the Royal Society (S.B.D. and M.S.-C.), the U.K. EPSRC, the Polish Academy of Sciences, the Japan Society for the Promotion of Science (R.J.W.), and CELTAM in Poland (M.S.-C.). This experiment was performed with the approval of the Japan Synchrotron Radiation Research Institute (JASRI) (Proposal No. 2004A0332-ND3a-np). We are indebted to the LACMS (Bristol) for access to their Beowulf cluster. We also thank H. Ebert for useful discussions, and Akiko Kikkawa (RIKEN/SPring-8) for characterization of the sample.

- 
- [1] G.L. Zhao and B.N. Harmon, Phys. Rev. B **45**, 2818 (1992).  
 [2] E.I. Isaev *et al.*, Solid State Commun. **129**, 809 (2004).

- [3] X. Huang, G.J. Ackland, and K.M. Rabe, Nat. Mater. **2**, 307 (2003).  
 [4] I.I. Naumov and O.I. Velikokhatniy, J. Phys. Condens. Matter **9**, 10 339 (1997).  
 [5] X. Y. Huang, I.I. Naumov, and K.M. Rabe, Phys. Rev. B **70**, 064301 (2004).  
 [6] C. Bungaro, K.M. Rabe, and A. DalCorso, Phys. Rev. B **68**, 134104 (2003).  
 [7] R.D. McDonald *et al.*, J. Phys. Condens. Matter **17**, L69 (2005); P.A. Goddard *et al.*, Phys. Rev. Lett. **94**, 116401 (2005).  
 [8] Z. Nishiyama, *Martensitic Transformation* (Academic Press, New York, 1978).  
 [9] S.M. Shapiro, B.X. Yang, Y. Noda, L.E. Tanner, and D. Schryvers, Phys. Rev. B **44**, 9301 (1991).  
 [10] W. Cochran, Adv. Phys. **9**, 387 (1960).  
 [11] P.W. Anderson, *Fizika Dielektrikov*, edited by G.I. Skanavi (Acad. Nauk. SSR, Moscow, 1960).  
 [12] J.A. Krumhansl and R.J. Gooding, Phys. Rev. B **39**, 3047 (1989).  
 [13] S.M. Shapiro, J.Z. Larese, Y. Noda, S.C. Moss, and L.E. Tanner, Phys. Rev. Lett. **57**, 3199 (1986).  
 [14] R. Bruinsma, Phys. Rev. B **25**, R2951 (1982).  
 [15] G.L. Zhao *et al.*, Phys. Rev. B **40**, 7999 (1989).  
 [16] G.L. Zhao and B.N. Harmon, Phys. Rev. B **48**, 2031 (1993).  
 [17] Y.-Y. Ye, Y. Chen, K.-M. Ho, B.N. Harmon, and P.A. Lindgard, Phys. Rev. Lett. **58**, 1769 (1987).  
 [18] W. Kohn, Phys. Rev. Lett. **2**, 393 (1959).  
 [19] G.M. Stocks *et al.*, in *Ordered Intermetallics—Physical Metallurgy and Mechanical Behavior*, edited by C.T. Liu *et al.* (Kluwer Academic Publisher, Dordrecht, 1992), pp. 15–36.  
 [20] N. Shiotani *et al.*, J. Phys. Soc. Jpn. **73**, 1627 (2004).  
 [21] M.J. Cooper, Rep. Prog. Phys. **48**, 415 (1985).  
 [22] H. Ebert, in *Electronic Structure and Physical Properties of Solids*, edited by H. Dreyssé, Lecture Notes in Physics Vol. 535 (Springer, Berlin, 1998), p. 191; <http://olymp.cup.uni-muenchen.de/ak/ebert/SPRKKR/>  
 [23] N. Hiraoka, M. Itou, T. Ohata, M. Mizumaki, Y. Sakurai, and N. Sakai, J. Synchrotron Radiat. **8**, 26 (2001).  
 [24] Y. Sakurai and M. Itou, J. Phys. Chem. Solids **65**, 2061 (2004).  
 [25] G. Kontrym-Sznajd, A. Jura, and M. Samsel-Czekala, Appl. Phys. A **74**, 605 (2002).  
 [26] N. Sakai, J. Phys. Soc. Jpn. **56**, 2477 (1987).  
 [27] G. Kontrym-Sznajd and M. Samsel-Czekala, Appl. Phys. A: Mater. Sci. Process. **70**, 89 (2000).  
 [28] D.G. Lock, V.H.C. Crisp, and R.N. West, J. Phys. F **3**, 561 (1973).  
 [29] Zs. Major *et al.*, Phys. Rev. Lett. **92**, 107003 (2004).